Journal of Electrical Engineering, Vol. 77, No. 1, 2026, pp. 1-9
https://reference-global.com/journal/JEE

Parametric short-circuit force analysis of three-phase busbars with multiple subconductors per main conductor

Dimitrios G. Triantafyllidis[1*], Georgios T. Andreou[2], Dimitris P. Labridis[2]

Four three-phase busbar configurations are examined, consisting of one, two, three and four subconductors per phase. The busbars are considered to be straight and rigid, carrying short-circuit currents in the steady-state condition, with a peak value equaling the peak value of the short-circuit current. The electromagnetic forces acting on the center of mass of each busbar are calculated using the Finite Element Method for solving the electromagnetic field diffusion equation. The outcome is compared to results computed according to the IEC Standard 865/93. 1216 arrangements have been considered, covering the complete corresponding range of the IEC Standard. The procedure has been fully automated in all stages, from the creation of the initial Finite Element Triangulations up to the post processing result extraction.

Keywords: busbars, electromagnetic forces, short-circuit current, finite element method, neural networks

1 Introduction

Electromagnetic forces induced in busbar conductors (Fig. 1) subjected to short circuit currents may lead to extremely hazardous conditions for personnel and apparatus. A confident estimation of the acting forces is essential to the system designer to take into consideration the required busbar support layout. Calculations for the instigated forces based on the IEC Standard 865/93 [1] are made under the assumption that the conductors are filamentary. To compensate for this assumption an effective distance between the main conductors is proposed.

In [2] the Finite Element Method (FEM) is used to solve the electromagnetic diffusion equation and calculate the entire information for the field, current and distribution of forces, for two specific busbar configurations, thus avoiding the necessity to assume filamentary conductors. This work showed good agreement between FEM-based calculations and the IEC Standard 865/93 in the case of one subconductor per main conductor (i.e., one subconductor per phase). In the second case examined, consisting of four subconductors per main conductor (i.e., four subconductors per phase) a significant difference between FEM calculations and the IEC Standard could be demonstrated.

Similar approaches implementing FEM in two or three dimensions have been proposed in [3-6]. In [7] a numerical and analytical modeling of busbar systems is proposed, investigating cases with multiple nonadjacent subconductors.

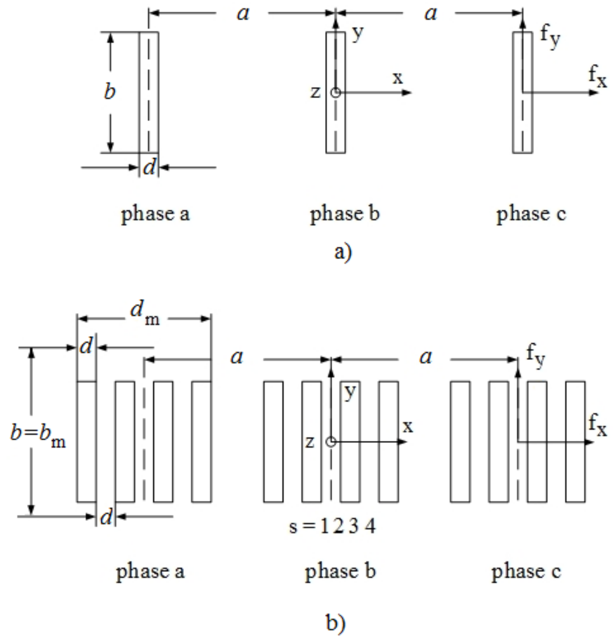

Fig. 1. Cross section of rigid busbars: a) one subconductor per main conductor, b) multiple subconductors per main conductor (s=1, 2, 3, 4)

In [8], a comparison has been made between the results obtained using FEM and calculations based on the IEC Standard 865/93 for a variety of one subconductor

[1]Department of Industrial Engineering and Management, International Hellenic University, 574 00 Sindos, Greece
[2]School of Electrical and Computer Engineering, Aristotle University of Thessaloniki, 541 24 Thessaloniki, Greece
*Corresponding author: drdimitri@ihu.gr

https://doi.org/10.2478/jee-2026-0001, Print (till 2015) ISSN 1335-3632, On-line ISSN 1339-309X

per main conductor busbar arrangements, covering the complete range of possible configurations of the IEC Standard.

For this purpose a fully automated mesh generation procedure, based on Let-It-Grow Neural Networks had been implemented [9], in order to generate 304 triangular meshes for all possible combinations of 16 α/d and 19 b/d ratios (Fig. 1). These meshes were then used as a starting point for an automated repetitive adaptive refinement procedure [10], based on the local error estimator of the discontinuity of the instantaneous tangential components of the magnetic field. The results showed very good agreement with the IEC Standard in all cases, regarding the main middle conductor.

Although a good agreement of results between the FE Method and the IEC Standard could be shown, nevertheless, in [8] forces acting on the outer conductors where not examined, whilst the present work introduces new correction factors even for these cases, but more important, in [2] and in [8] no parametric analysis of busbar arrangements with multiple subconductors per main conductor was carried out.

The present work addresses these cases by examining arrangements of up to four subconductors per main conductor for all possible combinations of 16 α/d_m and 19 b/d_m ratios (Fig. 1). In addition, the original cases presented in [8] are investigated again, producing a total number of 1216 busbar arrangements, in order to produce a complete dataset, including the outer conductors, which were not addressed in the previous work. Results of the present work are in good agreement with the original results, for the case of the center conductor with one subconductor per main conductor, albeit a better convergence of FEM with the present computational resources can be manifested.

Furthermore, significant deviations between FEM and the IEC Standard have been discovered in the cases of more than one subconductor per main conductor. Also, in all cases, including one subconductor per main conductor, significant differences between the two methods have been calculated for the outer main conductors. Although, the maximum force will always be acting on the middle conductor, hence a calculation of the forces on the outer conductors appears superfluous; the present work attempts to highlight the shortcomings of the traditional methods and therefore includes these cases as well.

2 Busbar arrangements

The busbars are considered rigid, positioned in parallel and in a single plane in free space (Fig. 1). The distance between main conductors α is regarded as minimal, compared to their length, so that the problem may be considered as two dimensional.

In addition, the following assumptions are made:

- The short-circuit fault examined is symmetrical in all three phases since it causes the greatest dynamic stress [11].
- The magnetic permeability μ is constant because only copper or aluminum busbars are used in installations and the busbars are positioned in free space, so there is no interaction with an iron enclosure.
- A steady state, balanced three-phase system of currents is applied to the main conductors, having an RMS value I_{rms} corresponding to the peak value of the short-circuit current i_{p3} in the case of a balanced three-phase short circuit:

$$I_{\mathrm{rms}} = \frac{i_{\mathrm{p3}}}{\sqrt{2}} \tag{1}$$

These same assumptions are also applied by the related IEC Standard, only in the Standard the conductors are also regarded filamentary and an even current distribution among subconductors of each main conductor is assumed. By using FEM, these latter assumptions are no longer necessary, thus a more accurate solution of the problem is expected.

For the case of one subconductor per main conductor the following arrangements were considered: 16 α/d and 19 b/d values and all of their combinations, resulting in 304 cases (Tab. 1). The same configurations were used for the cases of multiple subconductors per main conductors, only d was replaced by d_m, as required by [1]. The height of the busbars remains b=b_m as can be seen in Fig. 1. Although the IEC Standard requires the use of the symbol b_m in multiple subconductor cases, it is omitted in this work for reasons of simplicity.

Table 1. Busbar arrangements examined

α/d (α/d_m)	1.1, 1.5, 2, 3, 4, 5, 6, 7, 8, 9, 10, 15, 20, 30, 40, 50
b/d (b/d_m)	0.1, 0.4, 0.6, 0.8, 1.0, 1.2, 1.5, 2.0, 2.6, 3.0, 3.5, 4.0, 5.0, 6.0, 8.0, 10.0, 12.0, 16.0, 20.0

The main conductors are excited by a balanced, sinusoidal 50 Hz system of currents, as follows:

$$\begin{aligned} I_{\mathrm{a}} &= \sqrt{2} \cdot I_{\mathrm{rms}} e^{\mathrm{j}0^{\mathrm{o}}} \\ I_{\mathrm{b}} &= \sqrt{2} \cdot I_{\mathrm{rms}} e^{\mathrm{j}-120^{\mathrm{o}}} \\ I_{\mathrm{c}} &= \sqrt{2} \cdot I_{\mathrm{rms}} e^{\mathrm{j}-240^{\mathrm{o}}} \end{aligned} \tag{2}$$

3 Computation of forces

In accordance with the IEC Standard 865/93, the maximum force per unit length F_{mb} acting on the centre of mass of the middle main conductor of Fig. 1 is calculated in relation to the geometrical configuration and the profile of the busbars, by proposing an effective distance a_{m} [1]:

$$F_{\mathrm{mb}} = \frac{\mu_0}{2\pi a_{\mathrm{m}}} \cdot \frac{\sqrt{3}}{2} i_{\mathrm{p3}}^2 \tag{3}$$

The effective distance a_{m} is calculated as

$$a_{\mathrm{m}} = \frac{a}{k_{1\mathrm{s}}} \tag{4}$$

In Eqn. (4) the correction factor $k_{1\mathrm{s}}$ is given in [1] either by means of a family of curves for various a/d and b/d ratios, covering the range presented in Tab. 1, or by an equation presented in [1, Annex A].

Forces acting on the outer main conductors are not calculated in [1], but the maximum forces per unit length may be calculated according to [2] and [11], by means of Eqn. (5):

$$F_{\mathrm{ma}} = F_{\mathrm{mc}} = \frac{\mu_0}{2\pi a_{\mathrm{m}}} \cdot \frac{3+2\sqrt{3}}{8} i_{\mathrm{p3}}^2 \tag{5}$$

In the present work the forces are calculated by using FEM in the same approach as in [8]. For this purpose, the correction factor $k_{1\mathrm{s}}$ is being replaced by the factor k_{FEM} in Eqn. (4), thus the effective distance will be given by:

$$a_{\mathrm{m}} = \frac{a}{k_{\mathrm{FEM}}} \tag{6}$$

A separate correction factor is introduced for each main conductor, as opposed to [8], where only the centre main conductor was considered. The forces acting on the centre of mass of each main conductor, using FEM, are given by:

$$F_{\mathrm{maFEM}} = \frac{\mu_0}{2\pi a} k_{\mathrm{FEM_a}} \cdot \frac{3+2\sqrt{3}}{8} i_{\mathrm{p3}}^2 \tag{7}$$

$$F_{\mathrm{mbFEM}} = \frac{\mu_0}{2\pi a} k_{\mathrm{FEM_b}} \cdot \frac{\sqrt{3}}{2} i_{\mathrm{p3}}^2 \tag{8}$$

$$F_{\mathrm{mcFEM}} = \frac{\mu_0}{2\pi a} k_{\mathrm{FEM_c}} \cdot \frac{3+2\sqrt{3}}{8} i_{\mathrm{p3}}^2 \tag{9}$$

Correction factors $k_{\mathrm{FEM_a}}$, $k_{\mathrm{FEM_b}}$ and $k_{\mathrm{FEM_c}}$ for each main conductor are calculated by computing the forces F_{maFEM}, F_{mbFEM} and F_{mcFEM} and then by solving Eqns. (7-9) for the respective correction factor. The correction factors are computed for the range of values presented in Tab. 1 and compared to the correction factors used in Eqns. (3-5). In the case of FEM, the correction factor $k_{\mathrm{FEM_a}}$ is considered to be different than $k_{\mathrm{FEM_c}}$, as opposed to [2] and [11] (Eqn. (5)), where forces acting on the outer main conductors are considered equal. This assumption of symmetry may be justified for cases with one subconductor per main conductor, but in the case of multiple subconductors it does not apply, since current distribution among subconductors is not expected to be equal. This is also supported by the results presented in the next chapter.

4 Results

For all cases described in Tab. 1 a symmetrical system of currents according to Eqns. (2) has been applied to the main conductors. I_{rms} has been taken as 1000 A, 50 Hz, although the magnitude of the current is relevant only when the absolute value of the induced forces is sought for. For the calculation of the correction factors $k_{\mathrm{FEM_a}}$, $k_{\mathrm{FEM_b}}$ and $k_{\mathrm{FEM_c}}$ the magnitude I_{rms} is irrelevant, because the magnetic permeability is constant, as the arrangement of busbars is considered to be located in free space and no ferromagnetic materials are present to introduce nonlinearities. The percentage difference between the factors calculated by FEM and the factor $k_{1\mathrm{s}}$ has been calculated:

$$\%\text{Difference for conductor a} = \frac{k_{\mathrm{FEM_a}} - k_{1\mathrm{s}}}{k_{1\mathrm{s}}} \cdot 100 \tag{10}$$

$$\%\text{Difference for conductor b} = \frac{k_{\mathrm{FEM_b}} - k_{1\mathrm{s}}}{k_{1\mathrm{s}}} \cdot 100 \tag{11}$$

$$\%\text{Difference for conductor c} = \frac{k_{\mathrm{FEM_c}} - k_{1\mathrm{s}}}{k_{1\mathrm{s}}} \cdot 100 \tag{12}$$

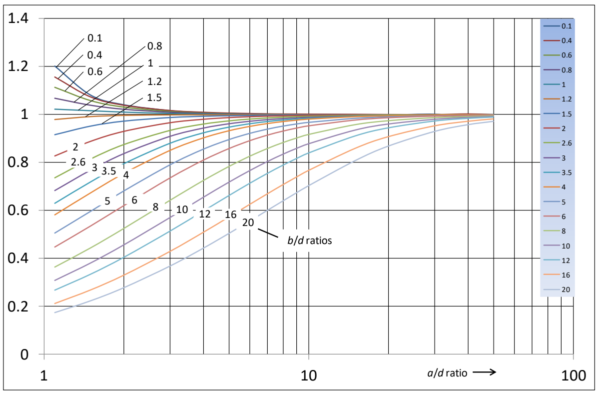

Fig. 2. Correction factor k_{FEM_a} for one subconductor per phase

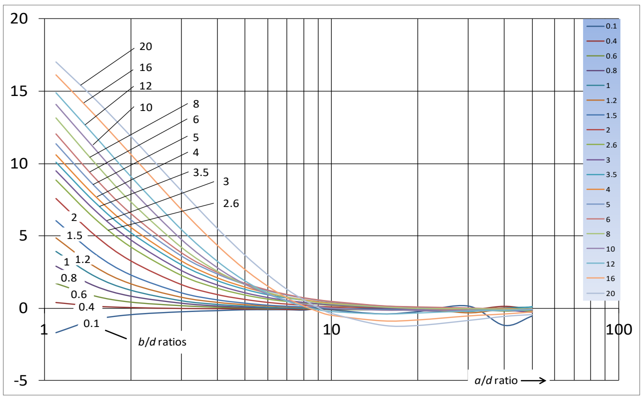

Fig. 5. % Difference for conductor a and one subconductor per phase

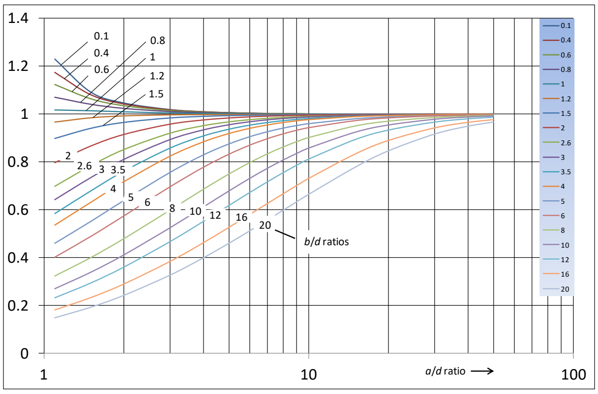

Fig. 3. Correction factor k_{FEM_b} for one subconductor per phase

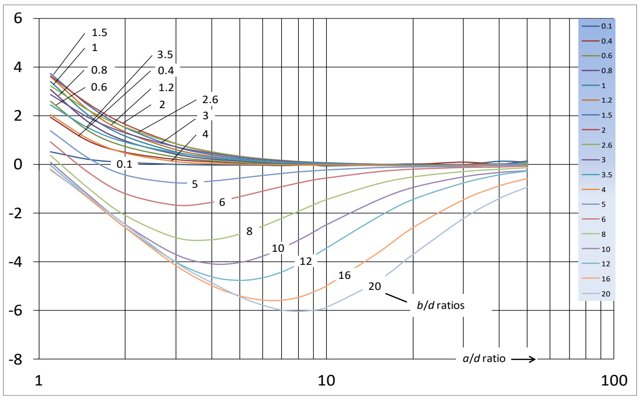

Fig. 6. % Difference for conductor b and one subconductor per phase

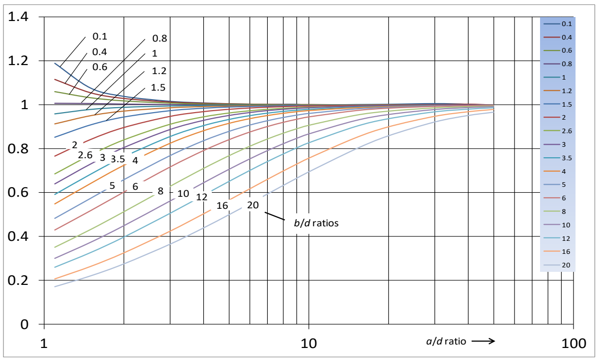

Fig. 4. Correction factor k_{FEM_c} for one subconductor per phase

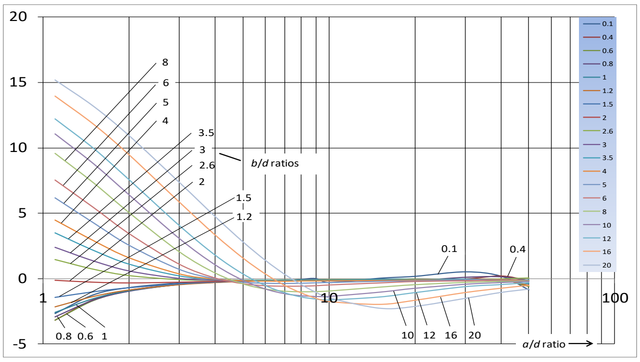

Fig. 7.. % Difference for conductor c and one subconductor per phase

Results for one subconductor per main conductor are presented in Figs. 2-4. The respective differences are demonstrated in Figs. 5-7. As can been seen from Fig. 6, the % differences between k_{FEM_b} and k_{1s} for the middle conductor are within the (–6%, 2%) range, which is larger than the differences calculated with the same method in [8], where differences had shown to be within the (–1.6%, 1.6%) range. Nevertheless, the % differences presented in Fig. 13 of [8] show a tendency to converge to the values presented in Fig. 6 of the present paper. In [8], the maximum number of mesh nodes allowable by the computational resources available at that time, was in the order of 10000, while the meshes used in the present paper are in the order of 50000 nodes. This is a clear indication that computer memory limitations led to an underestimation of the % difference in [8], although within acceptable limits. Since FEM in the present work has been let to converge, until two consecutive repetitions led to minimal deviations and computer memory was still available to continue the convergence process, if necessary, it is obvious that the results presented here are on the accuracy verge of the method.

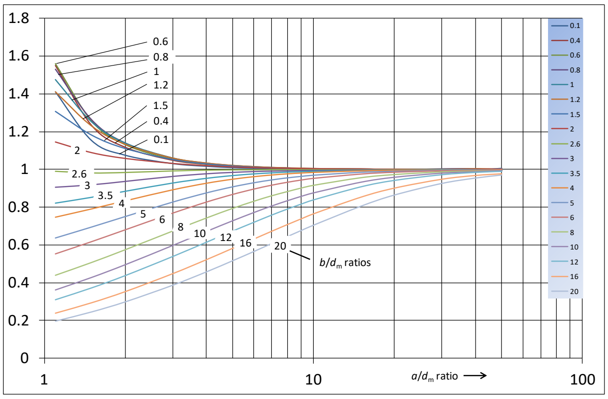

Fig. 8. Correction factor $k_{\mathrm{FEM_a}}$ for two subconductors per phase

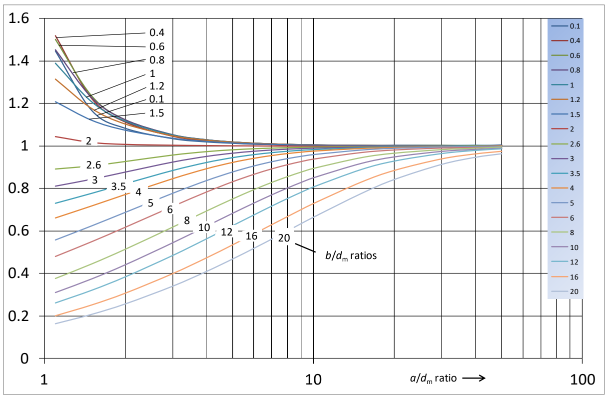

Fig. 9. Correction factor $k_{\mathrm{FEM_b}}$ for two subconductors per phase

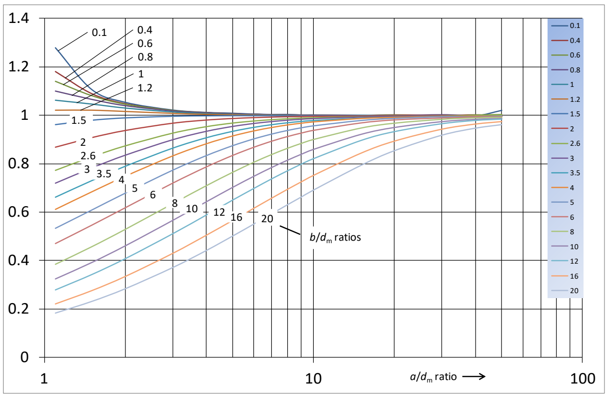

Fig. 10. Correction factor $k_{\mathrm{FEM_c}}$ for two subconductors per phase

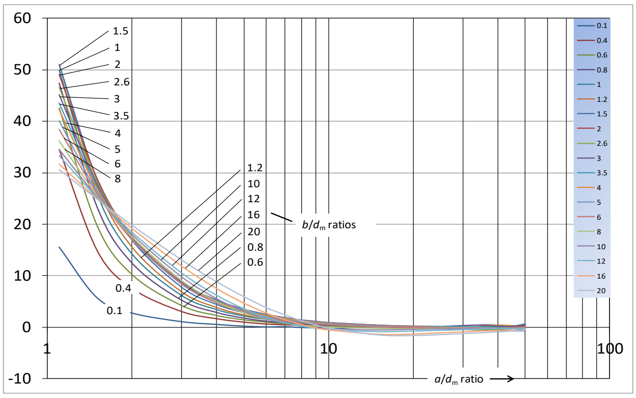

Fig. 11. % Difference for conductor a and two subconductors per phase

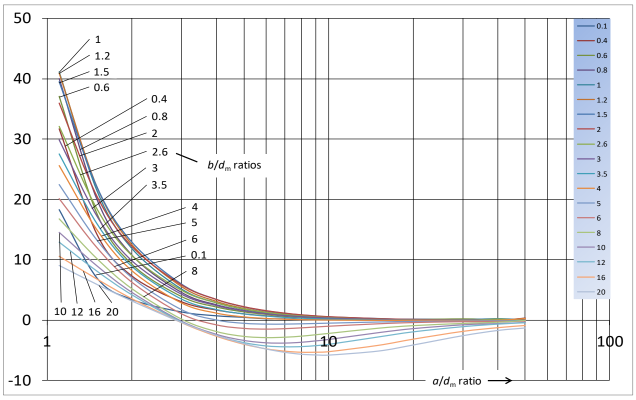

Fig. 12. % Difference for conductor b and two subconductors per phase

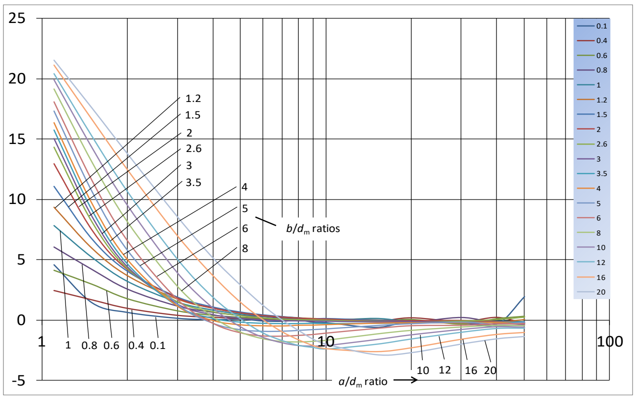

Fig. 13. % Difference for conductor c and two subconductors per phase

Results for two, three and four subconductors per main conductor (phase) can been seen in Figs. 8-13, Figs. 14-19 and Figs. 20-25, respectively.

The comparison of the results produced by FEM with the results obtained by the IEC Standard [1] and by [11], lead to the following conclusions:

1. The methods compared produce similar results in the case of the centre conductor with one subconductor per main conductor.
2. Even in the case of one subconductor per main conductor, significant differences can be found for the outer conductors.
3. In the case of multiple subconductors per main conductor, significant differences can be found for all three main conductors, regardless of position.

4. The differences are at their maxima when the α/d (α/d_m) ratio is at its minimum.
5. Differences vanish for large α/d (α/d_m) ratios.
6. Maximum percentage differences range from 15% in the case of one subconductor per main conductor to over 100% in the case of four subconductors per main conductor.

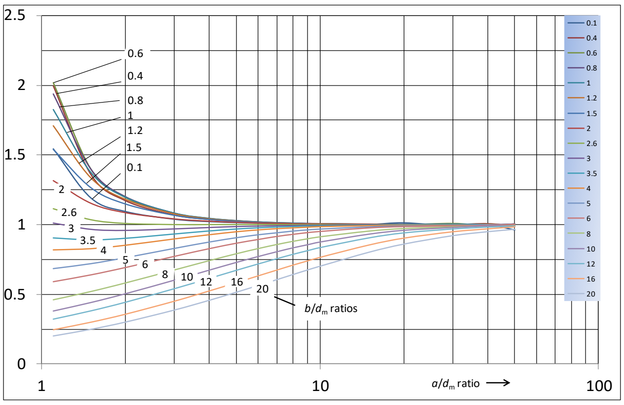

Fig. 14. Correction factor k_{FEM_a} for three subconductors per phase

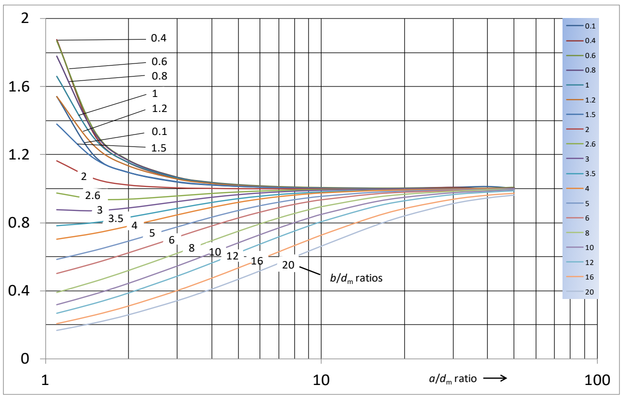

Fig. 15. Correction factor k_{FEM_b} for three subconductors per phase

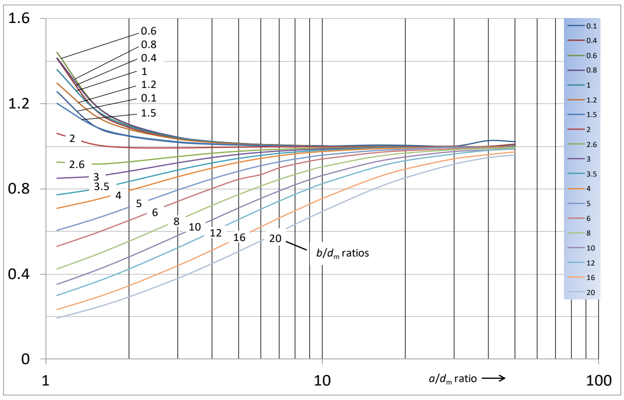

Fig. 16. Correction factor k_{FEM_c} for three subconductors per phase

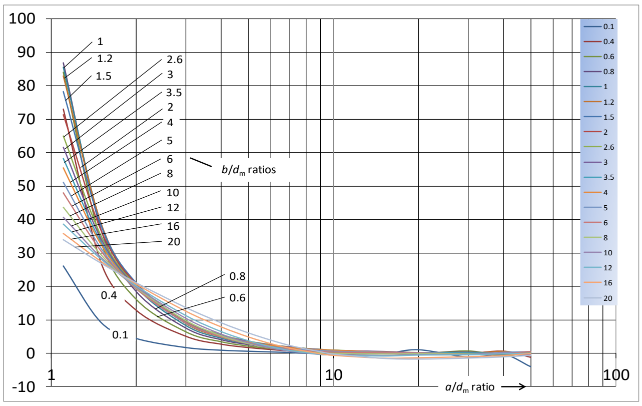

Fig. 17. % Difference for conductor a and three subconductors per phase

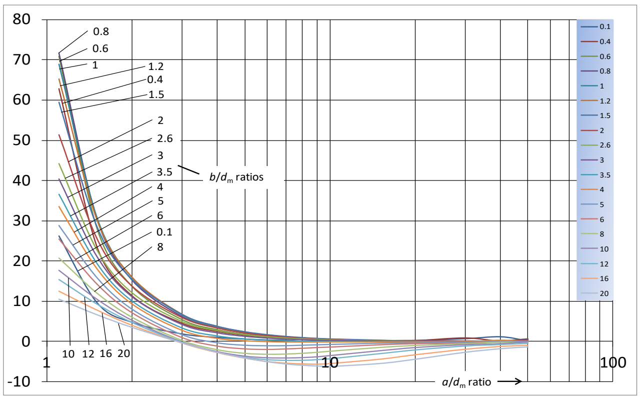

Fig. 18. % Difference for conductor b and three subconductors per phase

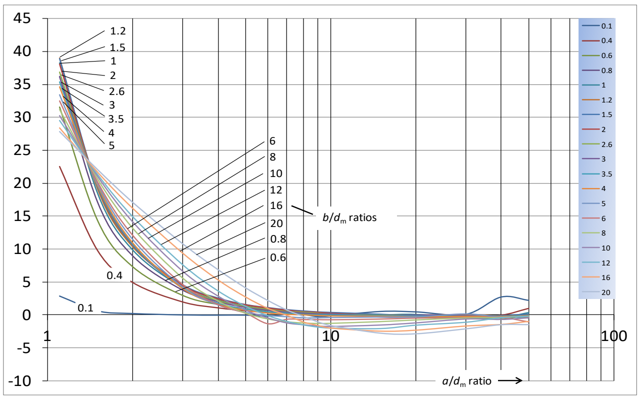

Fig. 19. % Difference for conductor c and three subconductors per phase

These conclusions could be expected by the fact that the reference methods [1] and [11] are based on the assumption of filamentary conductors. In particular, the unsymmetrical results produced by FEM in respect to the location of each main conductor, as opposed to the balanced results of the reference methods can be explained by the fact that the latter assume equal distribution of currents among subconductors. This is far from true, as the proximity effect is of important significance in this kind of busbar configurations, as has already been demonstrated in [2].

Results produced by FEM show a significant underestimation of the reference methods for forces acting on busbars under faulty conditions, reaching up to more than 100% in some extreme cases.

In practical configurations which are applied more often in the industry, this underestimation is lower, but still considerable high in some cases. In this aspect it is important to reconsider the method of calculating the correction factor k_{1s} as proposed in [1]. Results presented in the present work must be verified by other methods as well, in order to produce an updated IEC Standard, according to the new state of the art.

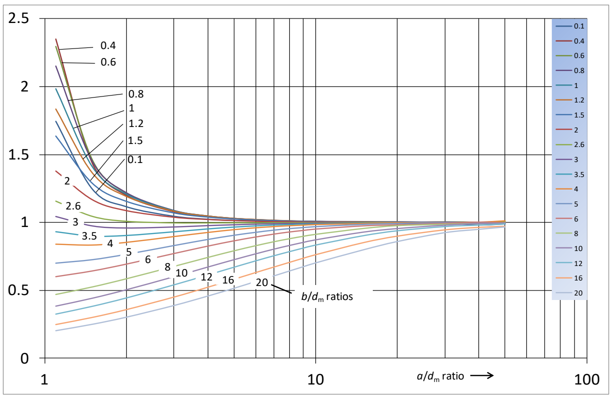

Fig. 20. Correction factor $k_{\mathrm{FEM_a}}$ for four subconductors per phase

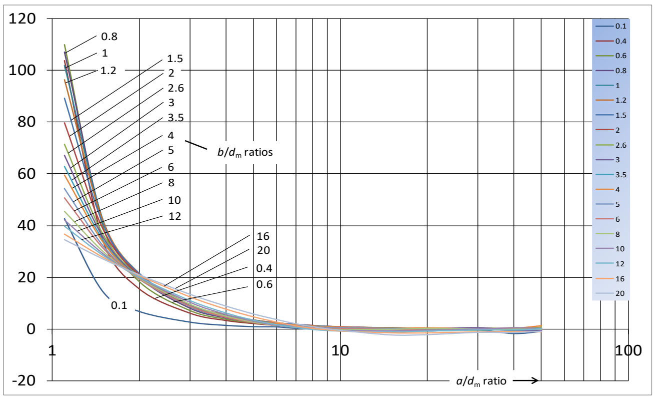

Fig. 23. % Difference for conductor a and four subconductors per phase

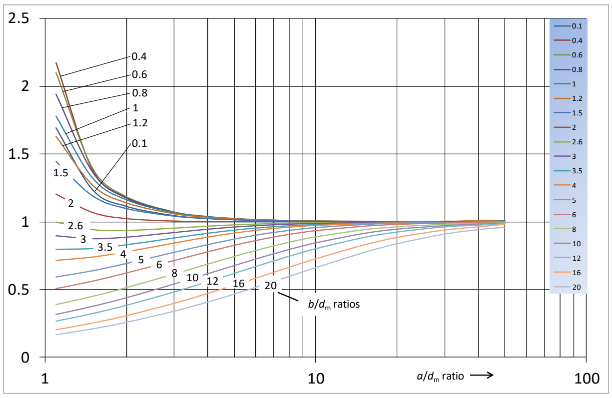

Fig. 21. Correction factor $k_{\mathrm{FEM_b}}$ for four subconductors per phase

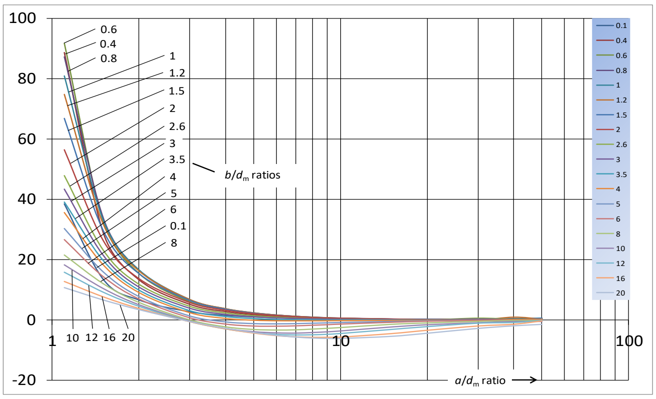

Fig. 24. % Difference for conductor b and four subconductors per phase

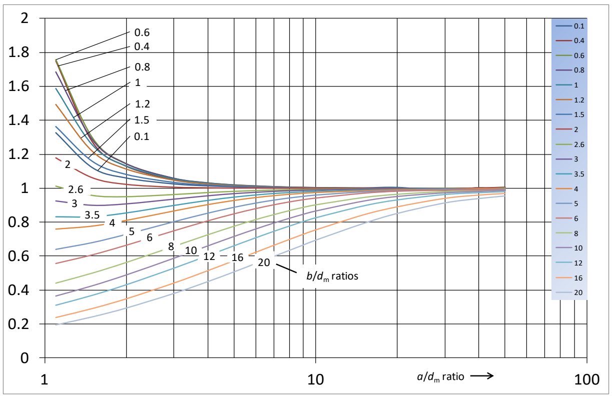

Fig. 22. Correction factor $k_{\mathrm{FEM_c}}$ for four subconductors per phase

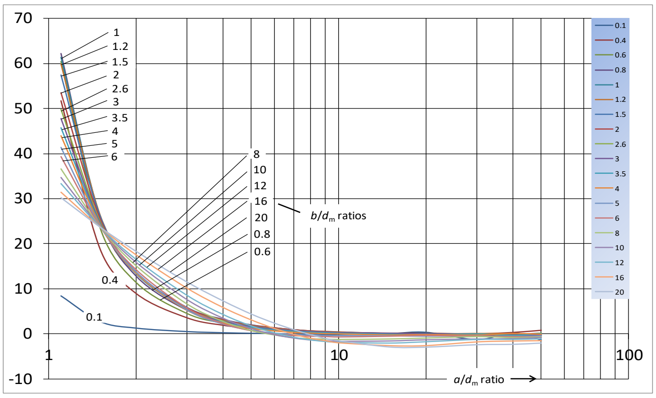

Fig. 25. % Difference for conductor c and four subconductors per phase

5 Calculation examples

Two cases will be examined, taken from examples 1 and 2 of [12]. Example 1 consists of a busbar system with one subconductor per main conductor. The distance between main conductors is a=0.2 m, the height of the busbars is b=60 mm and their width is d=10 mm. The current is i_{p3}=30.6 kA. For this configuration [12] proposes the value for k_{1s}=0.99, according to figure 1 of [1]. The exact value can be calculated to be k_{1s}=0.986, by using the formula in Annex A of [1], as corrected by the

1995 Corrigendum [13]. For this same case FEM calculates k_{FEM_b}=0.984, resulting in a slight underestimation by –0.203% of the computed force on the centre main conductor.

In example 2, the same configuration is used, albeit with three subconductors per main conductor of the same size as in example 1. k_{1s} can be calculated to have the exact value of 0.995, while k_{FEM_b}=1.032, resulting in a slightly higher calculated force by FEM by 3.72%.

In addition to these examples one more case is being examined (example 3) with the same configuration as in example 2, but with α=0.075 m. Calculations according to the reference methods are as follows:

$$\frac{a}{d_\text{m}} = \frac{0.075}{5 \cdot \left(\frac{10}{1000}\right)} = 1.5$$

$$\frac{b}{d_\text{m}} = \frac{60}{50} = 1.2$$

$$k_{1\text{s}} = 0.964$$

$$(3) \Rightarrow F_\text{mb} = 2084 \text{ N}$$

$$(5) \Rightarrow F_\text{ma} = F_\text{mb} = 1944 \text{ N}$$

FEM produces the following results: k_{FEM_a}=1.34, k_{FEM_b}=1.25, and k_{FEM_c}=1.15 resulting in forces which are significantly larger than the forces calculated by the reference methods. An overview of the results can be found in Tab. 2.

Table 2. Calculation examples

	Example 1	Example 2	Example 3
k_{1s}	0.986	0.995	0.964
k_{FEMa}	-	-	1.34
k_{FEMb}	0.984	1.032	1.25
k_{FEMc}	-	-	1.15
F_{ma} (N)	-	-	1944
F_{mb} (N)	799	807	2084
F_{mc} (N)	-	-	1944
F_{maFEM} (N)	-	-	2696
F_{mbFEM} (N)	798	837	2712
F_{mcFEM} (N)	-	-	2315
% Diff. a	-	-	39.0
% Diff. b	-0.203	3.72	29.7
% Diff. c	-	-	19.3

6 Conclusions

In the present work the electromagnetic forces acting on the center of mass of the main conductors of busbars with multiple subconductors are calculated using FEM. Results are compared to forces computed according to the IEC Standard 865/93. 1216 arrangements have been considered, covering the complete corresponding range of the IEC Standard. The calculated forces were in good agreement with the IEC standard in the case of the center conductor with one busbar per phase. In all other cases, significant deviations have been discovered, especially in the outer busbars, when the busbar distance was low in relation to their height.

Results presented in the present work lead to a strong indication that the IEC Standard may require further investigation which could lead to a revision, according to new scientific data.

References

[1] International Electrotechnical Commission, *Short-Circuit Currents – Calculation of Effects. Part 1: Definitions and Calculation Methods*, IEC 865. Geneva: Bureau central de la CEI, 1993.

[2] D. P. Labridis and P. S. Dokopoulos, "Electromagnetic forces in three-phase rigid busbars with rectangular cross-sections," *IEEE Transactions on Power Delivery*, vol. 11, no. 2, pp. 793-800, 1996. doi: 10.1109/61.489336

[3] D. A. Bergeron and R. E. Trahan, Jr., "A static finite element analysis of substation busbar structures," *IEEE Transactions on Power Delivery*, vol. 14, no. 3, pp. 890-896, 1999. doi: 10.1109/61.772330

[4] T. Takeuchi, T. Yoshizawa, Y. Kuse, and H. Hama, "3-D nonlinear transient electromagnetic analysis of short-circuit electromagnetic forces in a three-phase enclosure-type gas-insulated bus," *IEEE Transactions on Magnetics*, vol. 36, no. 4, pp. 1754-1757, 2000. doi: 10.1109/20.877783

[5] S. L. Ho, Y. Li, X. Lin, H. C. Wong, and K. W. E. Cheng, "A 3-D study of eddy current field and temperature rises in a compact bus duct system," *IEEE Transactions on Magnetics*, vol. 42, no. 4, pp. 987-990, 2006. doi: 10.1109/TMAG.2006.871632

[6] S. L. Ho, Y. Li, X. Lin, E. W. C. Lo, K. W. E. Cheng, K. F. Wong, "Calculations of eddy current, fluid, and thermal fields in an air insulated bus duct system," *IEEE Transactions on Magnetics*, vol. 43, no. 4, pp. 1433-1436, 2007. doi: 10.1109/TMAG.2007.892454

[7] A. Canova and L. Giaccone, "Numerical and analytical modeling of busbar systems," *IEEE Transactions on Power Delivery*, vol. 24, no.3, pp. 1568-1578, 2009. doi: 10.1109/TPWRD.2009.2014270

[8] D. G. Triantafyllidis, P. S. Dokopoulos, and D. P. Labridis, "Parametric short-circuit force analysis of three-phase busbars – a fully automated finite element approach," *IEEE Transactions on Power Delivery*, vol. 18, no. 2, pp. 531-537, 2003. doi: 10.1109/TPWRD.2002.804570

[9] D. G. Triantafyllidis and D. P. Labridis, "A finite element mesh generator based on growing neural networks," *IEEE Transactions on Neural Networks*, vol. 13, no.6, pp. 1482-1496, 2002. doi: 10.1109/TNN.2002.804223

[10] D. P. Labridis, "Comparative presentation of criteria used for adaptive finite element mesh generation in multiconductor eddy-current problems," *IEEE Transactions on Magnetics*, vol. 36, no. 1, pp. 267-280, 2000. doi: 10.1109/20.822537

[11] G. Hosemann and D. Tsanakas, “Dynamic short-circuit stress of busbar-structures with stiff conductors. Parametric studies and conclusions for simplified calculation methods,” *Electra*, no. 68, pp. 37-64, 1980.

[12] International Electrotechnical Commission, *Technical Report – Examples of Calculation*, IEC 865-2. Geneva: Bureau central de la CEI, 1994.

[13] International Electrotechnical Commission, *Corrigendum*, IEC 865-1. Geneva: Bureau central de la CEI, 1995.

Dimitrios G. Triantafyllidis was born in Stuttgart, Germany, in 1972. He received his Dipl.-Eng. degree and the Ph.D. degree from the School of Electrical and Computer Engineering at the Aristotle University of Thessaloniki in 1996 and 2001 respectively. He has worked for several years in various engineering positions in the private as well as public sectors. From 2010 to 2019 he was an Assistant Professor at the Department of Automation at the Alexander Technological Educational Institute of Thessaloniki and since 2020 he has been an Associate Professor at the Department of Industrial Engineering and Management of the International Hellenic University. His research interests include finite elements, electric vehicles, power electronics and power systems engineering.

Georgios T. Andreou was born in Thessaloniki, Greece, in 1976. He received the Dipl.-Eng. and Ph.D. degrees in electrical and computer engineering from the Aristotle University of Thessaloniki, in 2000 and 2006, respectively. He is currently an Asst. Professor at the School of Electrical and Computer Engineering of the Aristotle University of Thessaloniki. His current research interests include the operation and protection of power distribution networks, demand side management and the clean energy transition.

Dimitris P. Labridis was born in Thessaloniki, Greece in 1958. He received the Dipl.-Eng. and the Ph.D. degrees from the School of Electrical and Computer Engineering, Aristotle University of Thessaloniki, Greece, in 1981 and 1989 respectively. Since 1990 he has been with the School of Electrical and Computer Engineering at the Aristotle University of Thessaloniki, where he is currently a Professor. His research interests are power system analysis with special emphasis on the simulation of transmission and distribution systems.

Received 22 August 2025